Journal of Medicinal and Aromatic Plant Sciences 43(1-2), 2021, 25-36

ORIGINAL RESEARCH ARTICLE

Bioassay-guided isolation and characterization of potential α-glucosidase inhibitors from the seeds of *Quassia indica* Gaetrn.

PRABHA B[1,#] • BIJI M[1,2,#] • MADHUKRISHNAN M[1,2] • SHERIN DR[3] • RESHMITHA TR[2,4] • SUNIL VARUGHESE[1,2] • MANOJKUMAR TK[3] • NISHA P[2,4] • RADHAKRISHNAN KV[1,2,*]

Article History

Received: June 12th, 2021
Revised: June 18th, 2021
Accepted: June 20th, 2021

Key Words

Molecular simulation studies
Quassia indica Gaetrn
Quassinoids
α-Glucosidase inhibitory activity

ABSTRACT

*Bioactivity-guided isolation afforded 10 compounds from the ethanolic extract of the seeds of Quassia indica including, four novel quassinoids namely; samaderin L (**6**), samaderin R (**7**), samaderoside L (**9**) and samaderoside R (**10**). The structures were illustrated based on 1D and 2D NMR data, HRESIMS and single-crystal X-ray analysis. Among the quassinoids, samaderoside R (**10**) displayed significant α-glucosidase inhibitory activity. Molecular simulation experiments proved that samaderoside R (**10**) effectively binds to the active sites of Saccharomyces cerevisiae (**3A4A**) and human maltase glucoamylase (N- and C-terminal: **2QMJ** and **3TOP**) enzymes.*

INTRODUCTION

Quassia indica Gaertn. (*Q. indica*, Synonym: *Samadera indica*) commanly recognized as Niepa bark tree, belongs to the family Simaroubaceae one of the important plant family being widely used by traditional healers as antihelminthic, anti-amoebic, antiviral, antileukemic, antifeedant, antituberculosis, anticancer and antimalarial agents (Iasmine et al., 2014). Several compounds such asquassinoids, alkaloids, and triterpenoids were isolated as major components from *Q. indica*, which possess antimalarial, insecticidal, growth-regulating activities, etc. (Kazuo et al., 1993; Kazuo et al.,1994, Isao et al., 1996).

Type 2 diabetes mellitus (T2DM) is a well-known chronic metabolic syndrome, characterized by hyperglycemia due to the impaired insulin secretion from the pancreatic β-cells and insulin resistance in target tissues (De Fronzo et al., 2015). The occurrence of T2DM is increasing at an alarming rate, and it is foreseen to upsurge 629 million by 2045 (IDF Report, 2017). One of the therapeutic approaches for the precluding T2DM is the inhibition of the α-glucosidase enzyme; which catalyzes the hydrolysis of glycoside bonds in oligosaccharides. Thus, its inhibition helps to control the postprandial hyperglycemia and consequently prevent diabetes and its associated complications (Martin et al., 1996). However, the common α-glucosidase inhibitors (acarbose,

*Corresponding author; E-mail: radhu2005@gmail.com
#These authors contributed equally
[1]Chemical Sciences and Technology Division, [4]Agroprocessing and Technology Division, CSIR-National Institute for Interdisciplinary Science and Technology, Thiruvananthapuram-695019, India
[2]Academy of Scientific and Innovative Research (AcSIR), Ghaziabad-201002, India
[3]Centre for Computational Modeling and Data Engineering, Indian Institute of Information Technology and Management, Thiruvananthapuram-695581, India
Doi: https://doi.org/10.62029/jmaps.v43i1.B

GRAPHICAL ABSTRACT

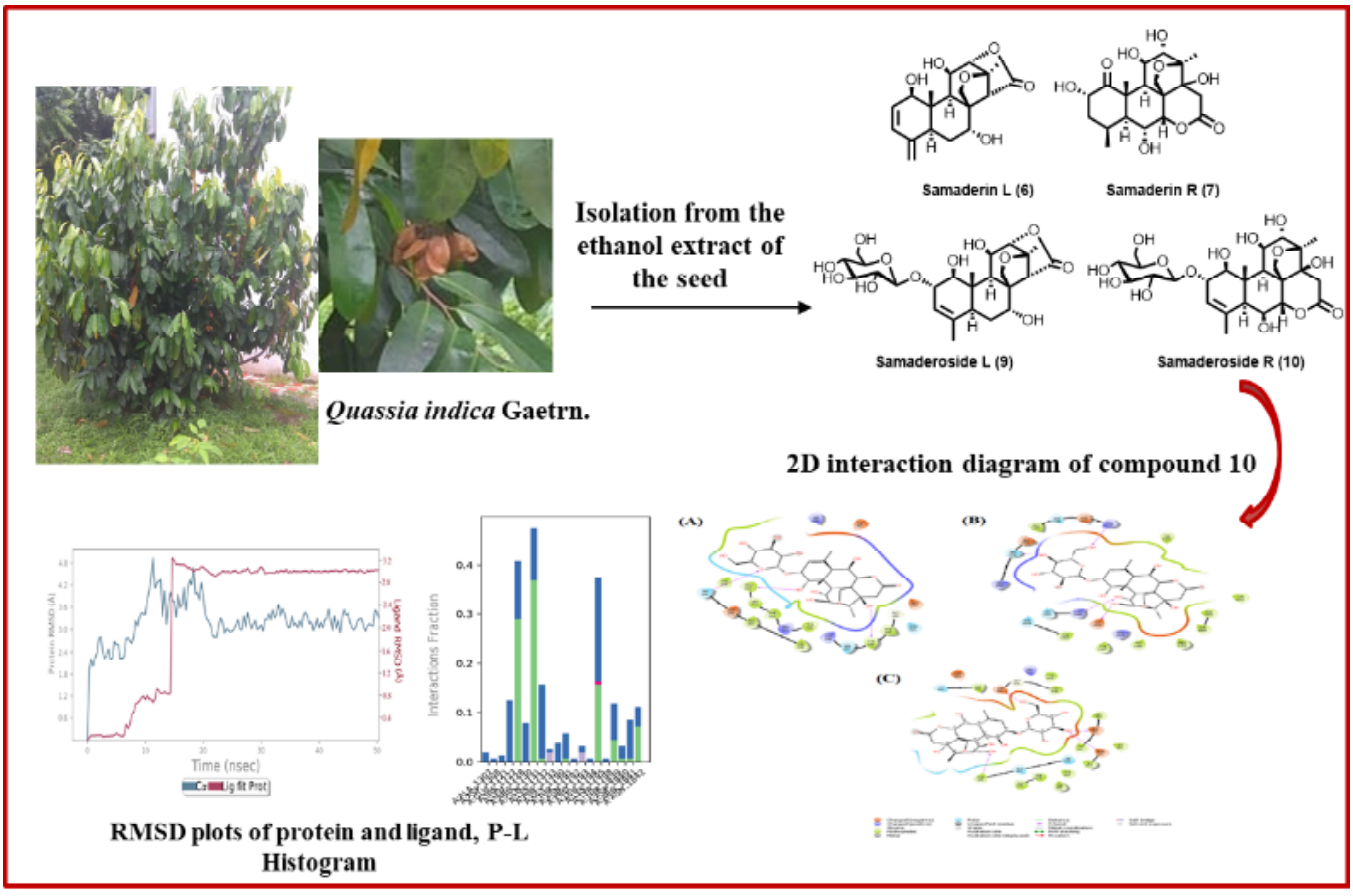

voglibose, and miglitol) successfully decrease the postprandial glucose level, but they are reported to cause many side effects like flatulence, diarrhea, renal failure and abdominal discomfort (Chougale et al., 2009). To assist this problem, compounds isolated from natural cradles have proven to be a valuable source for the development of promising antidiabetic drug lead. As part of our ongoing research to identify potential antidiabetic agent from natural resources (Greeshma et al., 2018; Prabha et al., 2018, 2019; Sasikumar et al., 2016, 2018, 2019) with less toxicity and high efficacy, we herein report the bioassay-guided isolation and characterization of α-glucosidase inhibitors from the seeds of *Q. indica*. Besides molecular simulation studies were also performed, to evaluate their mode of binding interaction with the active site of the enzymes.

MATERIALS AND METHODS

General experimental procedures and chemicals used

The melting points were recorded on a Büchi melting point apparatus. The infrared spectra were obtained using a Bruker FT-IR spectrometer, and values are acquired in cm^{-1}. 1D and 2D NMR spectra were recorded on a Bruker Avance 500 MHz, using $CDCl_3$, acetone-d_6 and DMSO-d_6 as solvents and the chemical shifts are expressed in (ppm) relative to the tetramethyl silane peak. The HRESIMS data were recorded at 60,000 resolutions using Thermo Scientific Exactive mass spectrometer. CC was done by silica gel (100-200 and 230-400 mesh; Merck, Darmstadt, Germany). Merck precoated silica gel F_{254} plates were used for thin-layer chromatography (TLC). Spots were detected on TLC under UV light or by heating after spraying samples with anisaldehyde-sulfuric acid mixture. α-Glucosidase from *Saccharomyces cerevesae*, acarbose and 4-nitrophenyl α-D-

glucopyranoside (*p*-NPG) was procured from M/s Sigma-Aldrich Chemicals (St. Louis, MO, USA). All the solvents used were of the highest grade available.

Plant material

Quassia indica Gaetrn. seeds were collected in October 2017 from the Alapuzha district of Kerala, India. A voucher specimen (**TBGT 81765**) was deposited in the herbarium of the Jawaharlal Nehru Tropical Botanical Garden and Research Institute (JNTBRI-Palode), Kerala, India.

Extraction and isolation

The seeds were cleaned, air-dried in a drier maintained at 50 °C and powdered. The powdered seed (300 g) was subjected to successive extraction using *n*-hexane, acetone, ethanol and water (1 L x 72 h x 3 times) at room temperature. After extraction, the solvent was removed under reduced pressure using Büchi rotary evaporator. The crude extract (28 g) was subjected to silica gel (100-200 mesh) CC using *n*-hexane, *n*-hexane-EtOAc gradient and EtOAc. Fractions of 200 mL each were collected and concentrated under reduced pressure.

The fraction pool 6 was again subjected to CC separation using 100-200 mesh sized silica gel with 40% *n*-hexane-EtOAc polarity, resulting in the isolation of compound **1** (13 mg) as a colourless solid. Fraction pool 8 was subjected to column chromatographic separation using 100-200 mesh sized silica gel with 50% *n*-hexane- EtOAc polarity resulted in the isolation of compound **2** (19 mg), as a colourless crystalline solid. The fraction pool 10 was subjected to column chromatographic separation using 100-200 mesh sized silica gel with 55% *n*-hexane- EtOAc polarity resulted in the isolation of compounds **3** (4 mg) and **4** (8 mg). Both of them were also obtained as colorless crystalline solids. Fraction pool 11 was subjected to column chromatographic separation using 100-200 mesh sized silica gel with 60% *n*-hexane-EtOAc polarity leading to the isolation of compound **5** (300 mg). By repeated column chromatography separation of fraction pool 13 using h-hexane-EtOAc polarity resulted in the isolation of compound **6** (2mg), compound **7** (21 mg) and compound **8** (11 mg) as colourless solids. Compound **9** (3 mg) and compound **10** (300 mg) were isolated as colourless amorphous solids from fraction pool 18 with 85% *n*-hexane-EtOAc and 90% *n*-hexane-EtOAc polarities respectively.

a-Glucosidase inhibitory activity

α-Glucosidase inhibitory activity was determined using a previous reported method with slight modification (Apostolidis et al., 2007).The samples (extracts and different concentrations of quassinoids) and 100 µL of α-glucosidase (*Saccharomyces cerevisiae*) solution (1.0 U/mL) in 0.1 M phosphate buffer (pH 6.9) were incubated for 10 min at room temperature. Followed by the addition of 250 µL *p*-nitrophenyl-α-D-gluco-pyranoside solution (5 mM) in 0.1 M phosphate buffer (pH 6.9) and the mixture was again incubated at 37 °C for 20 min. The reaction was stopped by adding 500 µL of Na_2CO_3. Here, acarbose was used as a positive control. Enzymatic activity was quantified by measuring absorbance at 405 nm using a multimode reader (Synergy 4 Biotek, USA) and the percentage of inhibition (IC_{50}) was calculated using the equation:

$$\% \text{ of inhibition} = \frac{\text{Absorbance of control - Absorbance of sample}}{\text{Absorbance of control}} \times 100$$

In silico studies

The preparation of the receptor and the ligands for docking, prediction of ADME/T (Absorption, Distribution, Metabolism, Excretion and Toxicity) properties, molecular docking and dynamics simulation studies were done by Schrodinger suite 2018-2. All the conformers of the eight quassinoids were generated by the LigPrep tool and then used for QikProp analysis to verify the pharmacokinetic parameters in order to predict the ADME/T properties. The values are compared with the range obtained from the QikProp manual. The crystal structures of isomaltase from *Saccharomyces cerevisiae* (PDB ID: **3A4A**) and the *N*-terminal and *C*-terminal of human maltase, glucoamylase (PDB ID: **2QMJ** and **3TOP** respectively) were retrieved from RCSB PDB (Protein Data Bank) (Sim et

al.,2008; Yamamoto et al., 2010; Ren et al., 2011).The prepared PDB files were further used for grid generation around the centroid of the workspace ligand 'acarbose'. Molecular docking of ligands with the receptors was carried out using the Glide programme of Schrodinger suite. The binding affinity of the ligands were predicted based on scoring functions- G-score (Glide score) and D-score (Dock score) using XP-visualizer. The pharmacophore model was generated using the Phase module of Schrodinger suite 2018-2. To predict the conformational stability of the protein-ligand complex, we carried out MD (Molecular Dynamics) simulation using the Desmond module of Schrodinger 2018 for 50 ns under OPLS-2005 force field. RMSD (Root Mean Square Deviation) plots for the backbone atoms for both protein and the ligand-bound protein were generated to understand the relative stability of the ligand inside the binding pocket of the protein. The P-L (Protein-Ligand) interaction histogram shows the interactions which favors the binding.

RESULTS AND DISCUSSION

Extraction, activity-oriented isolation and characterization of compounds

We initiated our studies with the preliminary *in vitro* α-glucosidase activity of different extracts of the dried and grounded seeds of *Q indica*. The results indicated that ethanol extract has significant inhibitory activity on α-glucosidase enzyme with IC_{50} value of 15.65 ± 0.70 *µ*g/mL (Acarbose: 45.37 ± 0.68 *µ*g/mL), followed by aqueous (41.02 ± 0.76 *µ*g/mL), *n*-hexane (45.14 ± 0.35 *µ*g/mL) and acetone (48.51 ± 0.49 *µ*g/mL) extracts. Thus, further isolation and purification was focused on the ethanol extract. The ethanol extract was subjected to various column chromatographic separation led to the isolation of ten compounds including four previously undescribed quassinoids, samaderin L (**6**), samaderin R (**7**), samaderoside L (**9**) and samaderoside R (**10**) along with six known quassinoids; samaderin A (**1**) (Philip et al., 2005), samaderin B (**2**) (Philip et al., 2005), samaderin C (**3**) (Isao et al., 1996), dihydrosamaderin B (**4**) (Kazuo et al., 1994), cedronin (**5**) (Philip et al., 2005) and brucein D (**8**) (Yaeko et al., 1989) (Figure 1).

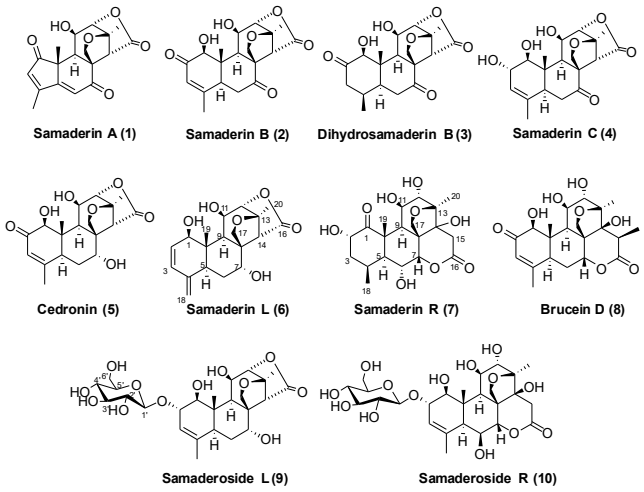

Figure 1: Chemical structures of phytochemicals isolated from *Q. indica*

Compound **6**, colorless solid [Mp: 271-273 °C; $[\alpha]^{25}_{D}$ +29° (*c* 0.2, MeOH)] gave a molecular formula of $C_{19}H_{24}O_6$ based on the HRESIMS [m/z 371.1469 $[M+Na]^+$, cal 371.1471 for $C_{19}H_{24}O_6Na$]. The IR absorption spectrum of compound **6** indicated the presence of a hydroxyl group (3421 cm^{-1}) and a γ-carbonyl lactone group (1756 cm^{-1}) of a C_{19}-type quassinoid. The ^1H NMR spectrum of compound **6** showed the presence of two tertiary methyls at δ_H 1.11 and 1.47 ppm (both 3H, s), four oxymethines [δ_H 4.62, 4.29, 4.23 and 3.90 ppm], and four olefinic protons at δ_H 6.12 (d, *J* = 10 Hz), 5.40 (d, *J* = 10 Hz), 4.89 (s) and 4.72 (s). The ^{13}C NMR spectrum displayed 19 signals including those for a γ-lactone carbonyl carbon [δ_C 173.8 ppm], six oxygen substituted carbons [δ_C 88.1, 84.0, 77.7, 75.1, 70.9 and 70.6 ppm] and four olefinic carbons [δ_C143.2,130.6, 129.8 and 112.0 ppm] (Table 1). The proposed structure of compound **6** was confirmed by HMBC, HMQC and ^1H-^1H COSY. In the HMQC spectrum, the protons at δ_H 4.89 and δ_H 4.72 ppm showed a correlation with δ_C 112.0 ppm, indicated an exo methylene group in ring A. The HMBC correlations (Figure 3) of Ha-18/C-3, C5 and Hb-18/C-3,C-5, confirmed the presence of an exomethylene at 4th position. The relative stereochemistry of compound **6** has been established by NOESY spectrum. The NOEs (Figure 3) between H-1/H-9, H-9/H-11, H-5/H-9, H-11/Me-20 certified the similar stereochemistry of H-1, H-5, H-9, H-11 and Me-20. Other NOESY

Table 1: ^{1}H and ^{13}C NMR data for **6** in $CDCl_3$ and **7** in CD_3COCD_3

	6		7	
Position	**^{1}H**	**^{13}C**	**^{1}H**	**^{13}C**
1	4.29 (brs, 1H)	77.7	-	215.5
2	5.40 (d, *J* = 10.0 Hz, 1H)	129.8	4.63-4.57 (m, 1H)	70.4
3	6.12 (d, *J* = 10.0 Hz, 1H)	130.6	2.21-2.16 (m, 1H) 1.08-0.95 (m, 1H)	50.0
4	-	143.2	2.28-2.24 (m, 1H)	30.6
5	2.64 (d, *J* = 12.5 Hz, 1H)	39.4	1.46 (t, *J* = 11 Hz & 10.5 Hz, 1H)	54.1
6	1.94 (dt, *J* = 14.0 & 3.0 Hz, 1H) 1.44 (m, 1H, merged with H-18)	29.6	3.80 - 3.76 (m, 1H, merged with H-17)	71.0
7	3.90 (brs, 1H)	70.6	4.73 (d, *J* = 2 Hz, 1H)	84.3
8	-	54.9	-	47.5
9	2.16 (d, *J* = 4.5 Hz, 1H)	43.9	2.31-2.29 (m, 1H)	38.6
10	-	43.5	-	53.0
11	4.62 (brs, 1H)	70.9	4.37-4.34 (m, 1H)	73.5
12	4.23 (brs, 1H)	84.0	4.46-4.45 (m, 1H)	70.5
13	-	88.1	-	84.2
14	2.62 (s, 1H)	59.7	-	81.3
15	-		3.63-3.60 (m, 1H) 2.37 (d, *J* = 19 Hz, 1H)	37.6
16	-	173.8	-	169.2
17	3.67 (d, *J* = 9.0 Hz, 1H) 4.49 (d, *J* = 9.0 Hz, 1H)	75.1	4.46-4.44 (m, H) 3.80-3.78 (m, 1H) merged with H-6	70.5
18	4.89 (brs, 1H) 4.72 (brs, 1H)	112.0	1.14 (d, *J* = 6 Hz, 3H)	22.8
19	1.11 (s, 3H)	10.6	1.62 (s, 3H)	17.0
20	1.47 (s, 3H)	21.0	1.18 (s, 3H)	17.2

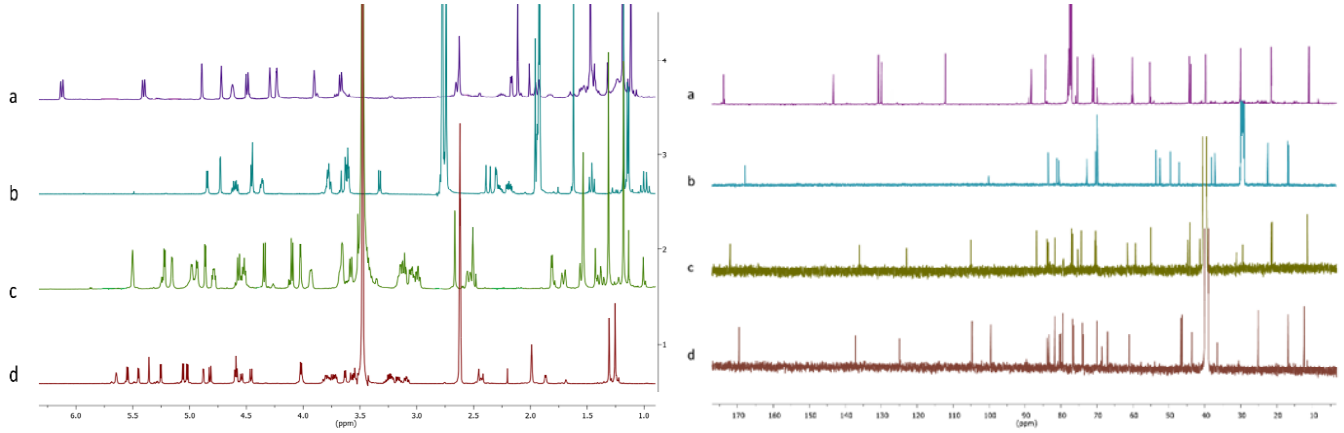

Figure 2: ^{1}H (left) and ^{13}C NMR (right) spectra of compounds. a) 6, b) 7, c) 9 and d) 10.

correlations H-19/Ha-16, H-7/Ha-17, H-7/H-14 and H-12/H-14 indicated the β-orientation of H-19, H-17, H-7, H-14 and H-12. Based on spectroscopic analysis, compound **6** was confirmed as a new C_{19} type quassinoid and named as Samaderin L.

Compound **7** was obtained as a colorless crystalline solid (Mp: 271-273 °C). The HRESIMS spectrum displayed a molecular ion at m/z 435.1631 $[M+Na]^+$ (calcd. for $C_{20}H_{28}O_9Na$, 435.1631) consistent with the chemical formula $C_{20}H_{28}O_9$. The IR spectra suggested the presence of hydroxyl (3410 cm^{-1}) and a γ-carbonyl lactone (1762 cm^{-1}). The compound **7** exhibited specific rotation at $[\alpha]_D^{25}$ +63.1° (*c* 0.3, MeOH). The ^{1}H NMR spectrum of compound **7**showed signals corresponding to an oxymethylene [δ_H4.45 and 3.80 ppm], four oxymethines [δ_H 4.73, 4.63-4.57, 4.38-4.35 and 3.75 ppm], two tertiary methyl groups [δ_H

Table 2: ^{1}H and ^{13}C NMR data for **9** and **10** in DMSO-d_6

	9		**10**	
Position	**^{1}H**	**^{13}C**	**^{1}H**	**^{13}C**
1	3.49 (m, 1H)	81.5	3.51 (d, *J* = 5.5 Hz)	80.4
2	3.93 (m, 1H)	83.7	3.63-3.60 (m, 1H)	80.0
3	5.50 (brs, 1H)	123.2	5.53 (brs, 1H)	124.9
4	-	136.4	-	137.2
5	2.54 (brd, *J* = 12.5 Hz, 1H)	40.8	2.32-2.30 (m, 1H)	46.3
6	1.71 (dt, J_1 = 13.5 Hz & J_2 = 2.5 Hz, 1H) 1.38 (td, J_1 = 13.0 Hz & J_2 = 2.0 Hz, 1H)	28.9	3.68-3.67 (m, 1H)	67.1
7	4.78 (m, 1H)	70.2	4.76 (d, *J* = 2 Hz, 1H)	83.4
8	-	54.6	-	46.7
9	1.81 (d, *J* = 4.5 Hz, 1H)	43.7	1.75 (d, *J* = 4.5 Hz, 1H)	43.6
10	-	44.4	-	46.4
11	3.66 (m, 1H)	69.9	4.47 (t, *J* = 6 and 5.5 Hz, 1H)	74.0
12	4.02 (d, *J* = 3.0 Hz, 1H)	83.3	3.90 (d, *J* = 5.5 Hz, 1H)	83.8
13	-	86.6	-	81.8
14	2.64 (s, 1H)	58.9	-	79.4
15	-		3.47-3.40 (m, 1H) 2.33-2.31 (m, 1H)	36.5
16	-	172.3	-	169.5
17	4.57 (d, *J* = 8 Hz, 1H) 3.58 (d, *J* = 8.5 Hz, 1H)	75.0	4.42 (d, *J* = 7 Hz, 1H) 3.61-3.59 (m, 1H)	68.6
18	1.54 (s, 3H)	20.8	1.87 (s, 3H)	25.2
19	1.18 (s, 3H)	10.9	1.19 (s, 3H)	12.4
20	1.31 (s, 3H)	20.7	1.14 (s, 3H)	16.8
1’	4.34 (d, *J* = 7.5 Hz, 1H)	105.3	4.34 (d, *J* = 7.5 Hz, 1H)	104.7
2’	2.98 (td, J_1 = 8 Hz & J_2 = 3.5 Hz, 1H)	74.1	2.97 (td, J_1 = 8 Hz & J_2 = 3.5 Hz, 1H)	73.8
3’	3.08 (m, 1H)	76.8	3.10 (m, 1H)	76.8
4’	3.04 (dd, J_1 = 9 Hz & J_2 = 5.5 Hz, 1H)	70.1	3.05 (dd, J_1 = 9 Hz & J_2 = 5.5 Hz, 1H)	70.1
5’	3.10-3.09 (m, 1H)	76.5	3.10-3.09 (m, 1H)	76.7
6’	3.71-3.65 (m, 1H) 3.47-3.40 (m, 1H)	61.1	3.70-3.65 (m, 1H) 3.48-3.42 (m, 1H)	61.1

1.18 and 1.62 ppm], and a secondary methyl groups [δ_H 1.14 (d, *J* = 6 Hz) ppm]. The ^{13}C NMR spectrum of **7** revealed 20 signals including those for carbonyl groups [δ_C 215.5 ppm], a γ-lactone carbonyl carbon [δ_C 169.2 ppm], seven oxygen substituted carbons [δ_C 84.2, 81.8, 81.3, 73.5 and 71.0 ppm] and methylene carbon [δ_C50.0 and 37.6 ppm] (Table 1). This is consistent with ^{1}H-^{1}H COSY, HMQC, HMBC and DEPT 135 experiments. The presence of the γ-carbonyl lactone function at C-16 was established by the HMBC experiment (Figure 3) with correlations from H-15. The stereochemistry of compound **7** was determined by NOESY spectrum(Figure 3). Furthermore, the correlations observed between H-5 and H-9, and H-11 indicated that these protons are in α-orientation. The correlations between H-6 and H-7 in the NOESY spectrum with small coupling constant revealed that the protons are in *â*-orientation. The structure was further unambiguously confirmed from its single-crystal X-ray analysis (CCDC Deposit Number: 2104307) (Figure 4). To the best of our knowledge, this is a novel C_{20} type quassinoid and named as samaderin R (**7**).

Compound **9** was obtained as colourless amorphous solid [Mp: 224-227 °C; $[\alpha]^{25}_{D}$ +32 ° (*c* 0.3, DMSO)]. The molecular formula was determined as $C_{25}H_{36}O_{12}$from HRESIMS [(m/z, 551.2113 $[M+Na]^{+}$; calcd. 551.2104) for $C_{25}H_{36}O_{12}Na$]. The IR spectrum of **9** indicated the

presence of hydroxyl group (3419 cm^{-1}) and lactone group (1753 cm^{-1}). The ^1H NMR spectrum showed an olefinic proton [δ_H 5.50 (s, 1H, H-3)], five oxymethines [δ_H3.49 (m, 1H, H-1), 3.93 (m, 1H, H-2), 4.78 (m, 1H, H-7), 4.02(d, *J* = 3 Hz, 1H, H-12) and 3.66 (m, 1H, H-11)], an oxymethylene [δ_H 4.57 and 3.58 (d, *J* = 8 Hz, each 1H, H-16)], one methylene [δ_H 1.71 (dt, J_1= 13.5 Hz and J_2= 2.5 Hz, 1H, Ha-6) and 1.38 (td, J_1= 13.0 Hz and J_2= 2.0 Hz, 1H, Hb-6)], three methyl groups [δ_H 1.54 (s, 3H, Me-17), 1.31 (s, 3H, Me-18) and 1.18 (s, 3H, Me-19)] and signals for a characteristic glucopranosyl moiety [δ_H 4.34 (d, *J* = 7.5 Hz, 1H, H-1'), 3.71-3.65 (m, 1H, Ha-6'), 3.47-3.40 (m, 1H, Hb-6'), 3.17-3.03 (m, 1H, H-3'), 3.07-3.02 (m, 1H, overlap, H-4'), 2.97 (td, J_1 = 8 Hz and J_2 = 3.5 Hz, 2')]. There were two olefinic signals [δ_C123.2 and 136.4 ppm], a carbonyl [δ_C172.3 ppm] and thirteen resonances for carbons bearing oxygen [δ_C105.3, 86.6, 83.7, 83.3, 81.5, 76.8, 76.5, 75.0, 74.1, 70.2, 70.1, 69.9 and 61.1 ppm] in the ^{13}C NMR (Table 2). The HMBC correlation between the anomeric proton H-1' and C-2 suggested that the gluco-pyranosyl unit was attached at the C-2 position and the coupling constant of anomeric proton 7.5 Hz typical of a β-anomer. The relative stereochemistry of **9** was assigned on the basis of NOESY spectrum (Figure 3).The cross-peaks of H-2/Me-19, H-7/H-14, H-12/H-14, H-16/H-7 and H-19/H-7 indicated that H-2, H-7, H-12, H-14, H-16 and Me-19 are cofacial and assigned as β-orientations, while the NOESY of H-1/H-5, H-1/H-9, H-9/H-11, Me-18/H-11 and H-5/H-9 showed that these protons are α-oriented. Based on the spectroscopic analysis, this is a novel quassinoid and named as samaderin L (9).

Compound **10** was isolated as a colorless amorphous solid (Mp: 285-288 °C), whose molecular formula was established as $C_{26}H_{38}O_{14}$,by HRESIMS [(m/z, 597.2157 $[M+Na]^+$; calcd. for $C_{26}H_{38}O_{14}Na$, 597.2159)]. Its IR spectrum displayed absorption bands, corresponding to hydroxyl (3421 cm^{-1}), δ-lactone (1723 cm^{-1}), and double bond (1662 cm^{-1}) moieties. The compound **10** exhibited specific rotation at $[\alpha]^{25}_D$ +70 ° (*c* 0.4, DMSO). The 1D and 2D NMR spectra are shown in the supporting information and ^1H and ^{13}C NMR are depicted in Table 2. The ^1H NMR and HMQC spectra of compound **10** revealed signals of an olefinic proton [δ_H 5.53 (s, 1H, H-3)],five oxymethines [δ_H4.47 (t, J_1 = 6 Hz and J_2 = 5.5 Hz, 1H, H-11), 3.90 (d, *J* = 5.5 Hz, 1H, H-6, H-12), 3.60-3.59 (dd, J_1= 7 Hz and J_2 = 4 Hz, 1H, H-1) and 3.47-3.42 (m, 2H, H-6 and H-7)], an oxymethylene [δ_H 4.43 and 3.63 (d, *J* = 7 Hz, each 1H, H-20)], one methylene [δ_H 3.47 and 2.34 (s, 1H each, H-15)], three methyl groups [δ_H 1.87 (s, 3H, H3-18), 1.19 (s, 3H, H3-19) and1.14 (s, 3H, H3-21)] and signals for a characteristic glucopranosyl moiety [δ_H 4.34 (d, *J* = 7.5 Hz, 1H, H-1'), 3.71-3.65 (m, 1H, H-6'), 3.47-3.40 (m, 1H, H-6'), 3.17-3.03 (m, 1H, H-3'), 3.07-3.02 (m, 1H, overlap, H-4'), 2.97 (td, J_1 = 8 Hz and J_2 = 3.5 Hz, 2')]. The ^{13}C NMR and DEPT spectra

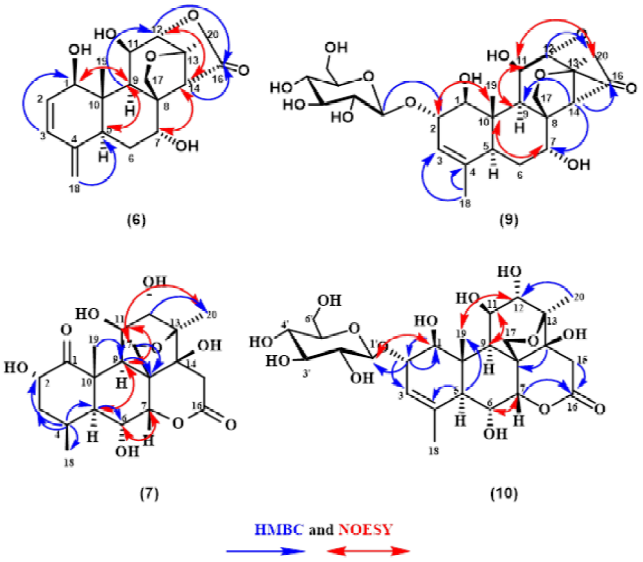

Figure 3: Key HMBC and NOESY correlations of compounds 6, 7, 9 and 10

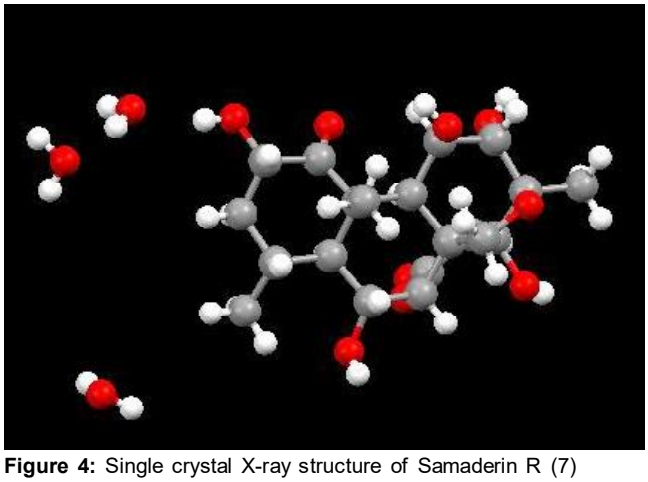

Figure 4: Single crystal X-ray structure of Samaderin R (7)

Table 3: *Saccharomyces cervease* α-glucosidase inhibitory activity of quassinoids isolated from *Q. indica*

Compounds	α-Glucosidase inhibitory activity (μM)
Samaderin A (**1**)	80.70 ± 0.53
Samaderin B (**2**)	123.70 ± 0.65
Dihydrosamaderin B (**3**)	259.01 ± 0.91
Samaderin C (**4**)	352.69 ± 0.78
Cedronin (**5**)	58.03 ± 0.23
Samaderin R (**7**)	59.96 ± 0.69
Brucein D (**8**)	66.39 ± 0.13
Samaderoside R (**10**)	48.50 ± 0.87
Acarbose	52.87 ± 0.22

Each value represents mean ± SD (standard deviation) from triplicate measurements

exhibited 26 carbon signals, including one carbonyl, one olefinic, three methyls, one methylene, three methines, four quaternary, and six saccharide-type carbons. The HMBC correlation (Figure 3) between the anomeric proton H-1' and C-2 and between H-2 and C-1' confirmed that the glucopyranosyl unit was attached at the C-2 position and must be a β-anomer, as suggested by the coupling constant (7.5 Hz) of the anomeric proton. The key HMBC and NOESY correlations are shown in Figure 3. The nuclear overhauser effect spectroscopy (NOESY) (Figure 3) cross peaks of H-2/Me-19, H-6/Me-19, H-7/H-14, H-7/Ha-20, H3-19/Ha-20, H-13/Hb-20, and H-14/Hb-20 indicated that H-2, H-6, H-7, H-13, H-14, and Me-19 are cofacial and assigned as β-orientations, while the NOESY of H-1/H-5, H-1/H-9, and H-5/H-9 showed that these protons are α-oriented. Therefore, the structure of compound **10** was elucidated as shown in **Figure 1** and named as samaderoside R.

α-Glucosidase inhibitory activity

As mentioned earlier, α-glucosidase is the major digestive enzyme found in the small intestine and they catalyze the release of glucose from polysaccharides. Recently, Abdulwali et al., reported the antidiabetic effects of *Brucea javanica*s seeds in type 2 diabetic rats. In that paper, the authors reported the α-glucosidase inhibitory activity of Brucein D (Abdulwali et al., 2017). Apart from this, there is no other report on the α-glucosidase inhibitory activity of quassinoids. Since compound **6** and **9** were obtained in trace amount, only the remaining compounds were taken for study. As shown in Table 3; some of the quassinoids exhibited moderate to significant inhibition of the α-glucosidase enzyme compared to the standard

Table 4: Pharmacokinetic parameters of compounds based on QikProp analysis

Properties	1	2	3	4	5	7	8	10
M.W.	330.337	362.379	364.394	364.394	364.394	412.436	408.447	574.578
#stars	0	1	1	0	0	0	0	1
#rotor	1	2	2	3	3	5	4	12
CNS	-1	-2	-2	-2	-1	-2	-2	-2
SASA	497.304	515.284	512.036	517.716	507.991	547.745	561.038	740.658
FISA	143.266	189.026	187.6	177.822	168.164	218.532	203.599	352.292
HBA	9.45	11.15	11.15	10.85	10.85	13.3	11.6	19.5
HBD	1	2	2	3	3	5	4	9
QPlogKhsa	-0.645	-0.669	-0.645	-0.541	-0.546	-0.638	-0.469	-1.294
HOA	3	2	3	2	2	2	2	3
% HOA	75.925	64.572	64.933	67.863	69.614	56.356	63.578	80
QPlogPo/w	0.303	-0.309	-0.289	-0.072	-0.053	-0.857	-0.056	-2.916
QPlogS	-2.028	-2.074	-2.032	-2.282	-2.728	-2.238	-2.651	-2.132
R Of Five	0	0	0	0	0	0	0	1

M.W. (Molecular Weight):130.0 to 725.0; #stars (few stars-more drug-like): 0 to 5; #rotor (Number of non-trivial and non-hindered rotatable bonds):0 to 15; CNS (Central Nervous System activity): -2 to +2; SASA (Total solvent accessible surface area in square angstroms): 300.0 to 1000.0 FISA (Hydrophilic component of total solvent accessable area): 7.0 to 333.0; HBA (Hydrogen bond acceptor): 2.0 to 20.0; HBD (hydrogen bond donor): 0.0 to 6.0; QPlogKhsa (binding to human serum albumin): -1.5 to 1.5; HOA (Human Oral Absorption): 1, 2, or 3 for low medium, and high; % HOA (Percent Human Oral Absorption): >80% is high, <25% is poor; QPlogPo/w (octanol/water partition coefficient):- 2.0 to 6.5; QPlogS (Aqueous solubility): -6.5 to 0.5; Ro5 (Number of violations of Lipinski's rule of five): maximum is 4.

Table 5: D-/G-score of quassinoids on 3A4A, QMJ and 3TOP proteins

Compounds	3A4A		2QMJ		3TOP	
	G-Score	D-Score	G-Score	D-Score	G-Score	D-Score
Samaderin A (**1**)	-4.16	-4.16	-3.05	-3.05	-3.83	-3.83
Samaderin B (**2**)	-5.11	-5.11	-2.26	-2.26	-5.3	-5.3
Dihydrosamaderin B (**3**)	-4.81	-4.81	-2.33	-2.33	-5.1	-5.1
Samaderin C (**4**)	-5.61	-5.61	-4.36	-4.36	-5.2	-5.2
Cedronin (**5**)	-6.88	-6.88	-3.38	-3.38	-4.79	-4.79
Samaderin R (**7**)	-6.65	-6.65	4.07	4.07	-5.88	-5.88
Brucein D (**8**)	-7.62	-7.62	-3.89	-3.89	-7.08	-7.08
Samaderoside R (**10**)	-8.88	-8.88	-8.07	-8.07	-8.19	-8.19

inhibitor, acarbose. Among them, samaderoside R (**10**) exhibited significant α-glucosidase inhibitory activity with IC_{50} value of 48.5 ± 0.87 μM, respectively.

Molecular simulation studies

To check the druggability of quassinoids from *Q. indica* by *in silico*, we carried out the QikProp analysis and found that all the quassinoids are more drug-like with few #stars value. The molecular weights of all of them are below 575 with an acceptable number of non-trivial and non-hindered rotatable bonds (#rotor, 0-15). All are less toxic to the central nervous system and having an appreciable range of hydrogen bond donors and acceptors. The solvent-accessible surface area (SASA) and its hydrophilic component (FISA) shows the binding ability of the ligands and their acceptance as drugs. The human oral absorption value indicates their oral absorptivity and binding to human serum albumin (QPlogKhsa, -1.5 to 1.5) increases its bioavailability, which is further confirmed by octanol/water partition coefficient, QPlogPo/w (-2.0 to 6.50) and aqueous solubility, QPlogS (-6.5 to 0.5). All the eight quassinoids are predicted as good candidates for antidiabetic drug development based on acceptable ADME/T with minimum violation from Lipinski Rule of Five (Ro5) (Table 4).

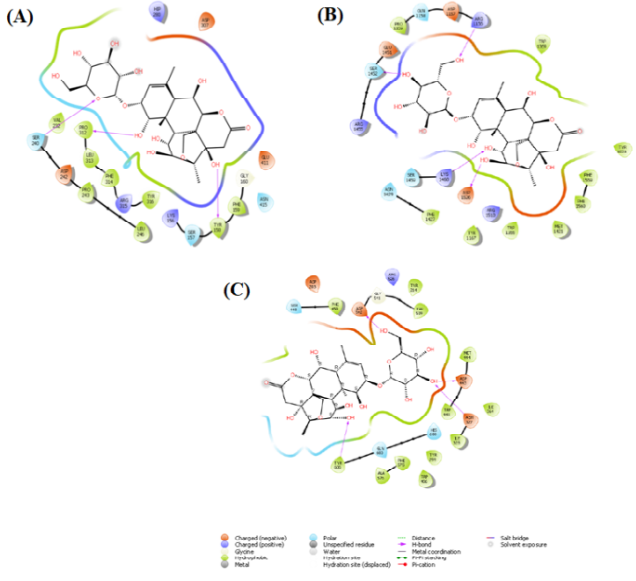

Figure 5: 2D interaction diagrams of samaderoside R (**10**) with (A) **3A4A** (B) **2QMJ** and (C) **3TOP** proteins

To visualize the probable binding modes of quassinoids on α-glucosidase enzymes, we carried out flexible docking simulations of selected receptors with isolated ligands. The crystal structures of isomaltase from *Saccharomyces cerevisiae* (PDB ID: **3A4A**) and the *N*-terminal and *C*-terminal of human maltase glucoamylase (PDB ID: **2QMJ** and **3TOP** respectively) were retrieved from RCSB PDB. First of all, we carried out the

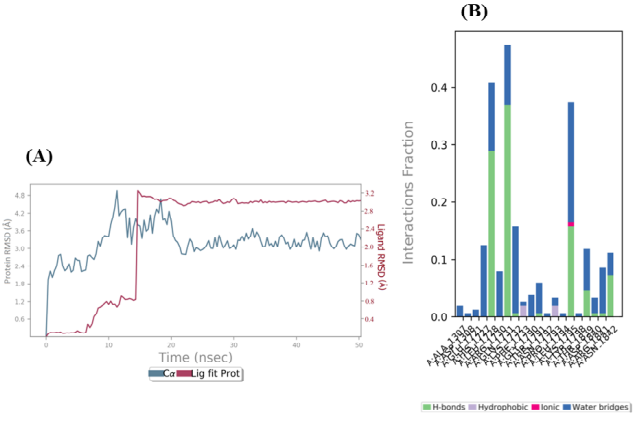

Figure 6: (A) Root mean square deviation of **3TOP** with samaderoside R (**10**) and (B) **3TOP** with samaderoside R (**10**) contacts

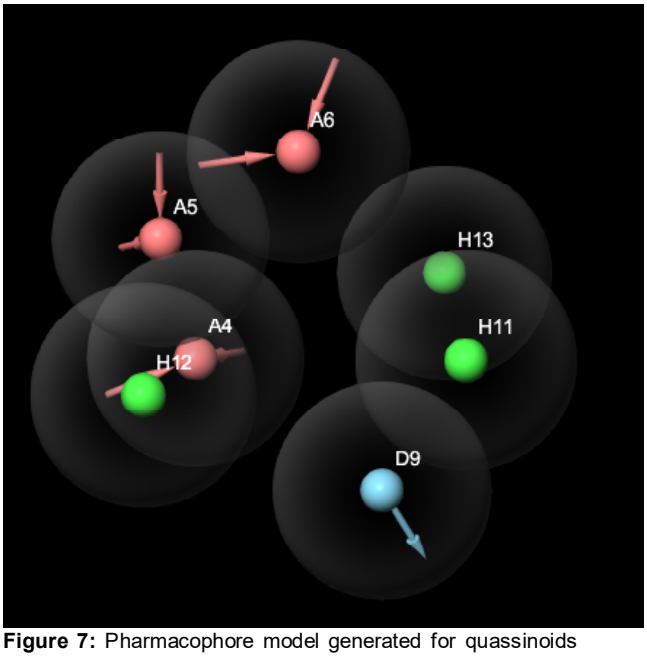

Figure 7: Pharmacophore model generated for quassinoids

docking simulations of eight quassinoids against **3A4A** and it was found that compound **10** shows better binding affinity with D-/G-score of -8.9 kcal/mol (Table5). The remaining quassinoids (**5, 7** and **8**) also shows better binding with scores less than -6.0 kcal/mol.

Consequently, we checked whether these quassinoids interacts with *N*- and *C*-terminal human maltase-glucoamylase (**2QMJ** and **3TOP** respectively**)**. Samaderoside R (**10**) [-8.1 kcal/mol] effectively binds with **2QMJ**, while others are not. Meanwhile, the *C*-terminal catalytic domains of human maltase glucoamylase (**3TOP**) show better interaction with Samaderoside R (**10**; G-/D-Score of -8.19 kcal/mol), followed by compound **8**(G-/D-score of -7.1) and compound **7** (G-/D-Score of -5.9kcal/mol). These results suggested that quassinoids (**5, 7, 8** and **10**) can act as a promising target for the treatment of T2DM. Further, it was clearer from docking data that the *C*-terminal provides the better binding pocket for the quassinoids in general. The 2D interaction diagrams of samaderoside (**10**) are shown in **Figure 5** and the G-/D-score of the isolated quassinoids are shown in Table 5.

With the aim of predicting the stability of the complex formed, we carried out the molecular dynamics simulations of **3TOP**-compound **10** complex under OPLS-2005 forcefield for 50 ns. It was found that the protein and ligand are stable under 3.0 Å after 20 ns, even though they deflect in the initial stage of trajectory. This stable complexation was further confirmed by P-L (Protein-Ligand) interaction histogram (Figure 6). The main interaction is H-bonding of Leu1728, Gln1731, Leu1794, Tyr1798 and Asn1842 and hydrophobic interactions of Pro1793 and Phe1733. The strong water bridges are also there to stabilize the complex formation.The pharmacophore hypothesis generates a model in which there are three H-bond acceptors, one H-bond donor and three hydrophobic regions (Figure 7).

CONCLUSION

In conclusion, phytochemical investigation of the seeds of *Quassia indica* led to the isolation of four novel quassinoids [samaderin L (**6**), samaderin R (**7**), samaderoside L (**9**) and samaderoside R (**10**)] along with six known quassinoids. Among the quassinoids, Samaderoside R (**10**) exhibited significant α-glucosidase inhibitory activity with IC_{50} value of 48.50±0.87 μM. The molecular simulation studies indicated that samaderoside R (**10**) effectively binds to the pocket of isomaltase from *Saccharomyces cerverce* (**3A4A**) and, *N*- (**2QMJ**) and *C*-(**3TOP**) terminal human maltase glucoamylase enzymes. Further studies are required to establish the therapeutic efficacy and safety of samaderoside R (**10**) as promising α-glucosidase inhibitors.

ACKNOWLEDGEMENTS

The authors acknowledge Mrs. Saumini Mathew and Mrs. S. Viji of CSIR-NIIST, India for recording NMR and HRESIMS spectra. The authors also acknowledge CSIR India, and UGC India,for research fellowship.

Declaration of Competing Interest

The authors declare that they have no known competing financial interests or personal relationships that could have appeared to influence the work reported in this paper.

REFERENCES

Adisakwattana S, Lerdsuwankij O, Poputtachai U, Minipun A, Suparpprom C. 2011. Inhibitory activity of cinnamon bark species and their combination effect with acarbose against intestinal α-glucosidase and pancreatic α-amylase. *Pl Food Hum Nutr* **66:**143-148.

Apostolidis E, Kwon YI, Shetty K. 2007. Inhibitory potential of herb, fruit, and fungal- enriched cheese against key enzymes linked to type 2 diabetes and hypertension. *Innov. Food Sci Emerg* **8**: 46-54.

Chougale AD, Ghadyale VA, Panaskar SN, Arvindekar AU.2009. Alpha-glucosidase inhibition by stem extract of *Tinospora cordifolia*. *J Enzyme Inhib Med Chem* **24**: 998-1001.

De Fronzo RA, Ferrannini E, Groop L, Henry RR, Herman WH, Holst JJ, Hu FB, Kahn CR, Raz I, Shulman GI, Simonson DC, Testa MA, Weiss R.2015. Type 2 diabetes mellitus. *Nat Rev Dis Primers* **1**: 1-22.

Friesner RA, Murphy RB, Repasky MP, Frye LL, Greenwood JR, Halgren TA, Sanschagrin PC, Mainz DT.2006. Extra Precision Glide: Docking and Scoring Incorporating a Model of Hydrophobic Enclosure for Protein-Ligand Complexes. *J Med Chem* **49:** 6177–6196.

Gopalan G, Prabha B, Joe A, Reshmitha TR, Sherin DR, Sabu M, Manojkumar T K, Radhakrishnan KV, Nisha P. 2019. Antidiabetic properties of apiforol, a potential lead isolated from the seeds of *Musa balbisiana*. *J Sci Food Agric* **99**: 2521-2529.

Halgren TA, Murphy RB, Friesner RA, Beard HS, Frye LL, Pollard WT, Banks JL.2004. Glide: A new approach for rapid, accurate docking and scoring. 2. enrichment factors in database screening. *J Med Chem* **47:** 1750–1759.

Iasmine ABSA, Henrique MM, Luiz ALS, Karina PR. 2014. Simaroubaceae family: botany, chemical composition and biological activities. *Rev Bras Farmacogn* **24**: 481-501.

International Diabetes Federation. (2017). from http://www.diabetesatlas.org

Isao K, Taifo M, Ko-ichi Y, Shinsaku N, Tadanori M, Motomasa K, Hirotaka S. 1996. Indonesian medicinal plants XVII. Characterization of Quassinoids from the stems of *Quassia indica. Chem Pharm Bull* **44**: 2009-2014.

Kazuo K, Taichi O.1993. Indaquassin A and B: Quassinoids from *Quassia indica. Phytochem* **34**: 505-509.

Kazuo K, Taichi O. 1994. Quassinoids from *Quassia indica. Phytochem* **35**: 459- 463.

Martin AE, Montgomery PA.1996. Acarbose: an alpha-glucosidase inhibitor. *Am J Health Syst Pharm* **53**: 2277-2290.

Prabha B, Neethu S, Lekshmy KS, Sherin DR, Madhukrishnan M, Ananthakrishnan R, Rameshkumar KB, Manojkumar TK, Jayamurthy P, Radhakrishnan KV. 2018. Antidiabetic potential of phytochemicals isolated from the stem bark of *Myristica fatua* Houtt. var. magnifica (Bedd.) Sinclair, *Bioorg Med Chem* **26**: 3461-3467.

Prabha B, Sini S, Sherin DR, Neethu S, Rameshkumar KB, Manojkumar TK, Jayamurthy P, Radhakrishnan KV.2018. Promalabaricone B from *Myristica fatua* Houtt. var. *magnifica* (Bedd.) Sinclair seeds demonstrate antidiabetic potential by inhibiting carbohydrate hydrolyzing enzymes, protein glycation and modulating glucose uptake via the activation of AMPK in L6 myotubes. *Nat Prod Res.* https://doi.org/10.1080/14786419.2019.1607852).

Philip HC, Naidoo D, Mulholland DA, Randrianarivelojosia M. 2005. Quassinoids from the leaves of the Madagascan Simaroubaceae *Samadera madagascariensis Phytochem* **66**: 2734-2739.

Ren L, Qin X, Cao X, Wang L, Bai F, Bai G, Shen Y.2011. Structural insight into substrate specificity of human intestinal maltase-glucoamylase. *Prot Cell* **2**: 827-836.

Sasikumar P, Prabha B, Reshmitha TR, Sheeba V, Pradeep AK, Rohit KR, Dhanya BP, Sivan VV, Jithin MM, Anil KN, Shibi IG, Nisha P, Radhakrishnan KV. 2016. Comparison of antidiabetic potential of (+) and (-) Hopeaphenol, a pair of enantiomers isolated from *Ampelocissus indica* (L.) and *Vateria indica* Linn, with respect to inhibition of digestive enzymes and induction of glucose uptake in L6 myotubes. *RSC Adv* **6**: 77075-77082.

Sasikumar P, Sharathna P, Prabha B, Varughese S, Kumar NA, Sivan VV, Sherin DR, Suresh E, Manojkumar TK, Radhakrishnan KV.2018. Dihydro-β,- agaro furan sesquiterpenoids from the seeds of *Celastrus paniculatus* Willd. and their α-glucosidase inhibitory activity. *Phytochem Lett* **26**: 1-8.

Sasikumar P, Lekshmy KS, Sini S, Prabha B, Kumar NA, Sivan VV, Jithin MM, Jayamurthy P, Shibil G, Radhakrishnan KV. 2019. Isolation and characterization of resveratrol oligomers from the stem bark of *Hopea ponga* (Dennst.) Mabb. and their antidiabetic effect by modulation of digestive enzymes, protein glycation and glucose uptake in L6 myocytes. *J Ethnopharmacol* **236**: 196-204.

Sim L, Quezada CR, Sterchi EE, Nichols BL, Rose DR. 2008. Human intestinal maltase-glucoamylase: crystal structure of the *N*-terminal catalytic subunit and basis of inhibition and substrate specificity. *J Mol Biol* **375**: 782-792.

Yamamoto K, Miyake H, Kusunoki M, Osaki S.2010. Crystal structures of isomaltase from *Saccharomyces cerevisiae* and in complex with its competitive inhibitor maltose. *Febs J* **277**: 4205-4214.